AD_____
(Leave blank)

Award Number:

W81XWH-07-1-0083

TITLE:
On-line Adaptive Radiation Treatment of Prostate Cancer

PRINCIPAL INVESTIGATOR:
Tiezhi Zhang

CONTRACTING ORGANIZATION:
William Beaumont Hospital
Royal Oak, Michigan

REPORT DATE:
January 2009

TYPE OF REPORT:
Annual

PREPARED FOR: U.S. Army Medical Research and Materiel Command
                Fort Detrick, Maryland   21702-5012

DISTRIBUTION STATEMENT: (Check one)

    √   Approved for public release; distribution unlimited

        Distribution limited to U.S. Government agencies only;
        report contains proprietary information

The views, opinions and/or findings contained in this report are
those of the author(s) and should not be construed as an official
Department of the Army position, policy or decision unless so
designated by other documentation.

REPORT DOCUMENTATION PAGE

Form Approved
OMB No. 0704-0188

Public reporting burden for this collection of information is estimated to average 1 hour per response, including the time for reviewing instructions, searching existing data sources, gathering and maintaining the data needed, and completing and reviewing this collection of information. Send comments regarding this burden estimate or any other aspect of this collection of information, including suggestions for reducing this burden to Department of Defense, Washington Headquarters Services, Directorate for Information Operations and Reports (0704-0188), 1215 Jefferson Davis Highway, Suite 1204, Arlington, VA 22202-4302. Respondents should be aware that notwithstanding any other provision of law, no person shall be subject to any penalty for failing to comply with a collection of information if it does not display a currently valid OMB control number. **PLEASE DO NOT RETURN YOUR FORM TO THE ABOVE ADDRESS.**

1. REPORT DATE	2. REPORT TYPE	3. DATES COVERED
31-01-2009	Annual	1 JAN 2007 - 31 DEC 2008

4. TITLE AND SUBTITLE	5a. CONTRACT NUMBER
On-line Adaptive Radiation Treatment of Prostate Cancer	W81XWH-07-1-0083
	5b. GRANT NUMBER
	5c. PROGRAM ELEMENT NUMBER

6. AUTHOR(S)	5d. PROJECT NUMBER
Tiezhi Zhang	
	5e. TASK NUMBER
	5f. WORK UNIT NUMBER
Email:	

7. PERFORMING ORGANIZATION NAME(S) AND ADDRESS(ES)	8. PERFORMING ORGANIZATION REPORT NUMBER
William Beaumont Hospital Royal Oak, Michigan	

9. SPONSORING / MONITORING AGENCY NAME(S) AND ADDRESS(ES)	10. SPONSOR/MONITOR'S ACRONYM(S)
U.S. Army Medical Research and Materiel Command Fort Detrick, Maryland 21702-5012	
	11. SPONSOR/MONITOR'S REPORT NUMBER(S)

12. DISTRIBUTION / AVAILABILITY STATEMENT
Approved for Public Release; Distribution Unlimited

13. SUPPLEMENTARY NOTES

14. ABSTRACT

None provided.

15. SUBJECT TERMS
None provided.

16. SECURITY CLASSIFICATION OF:			17. LIMITATION OF ABSTRACT	18. NUMBER OF PAGES	19a. NAME OF RESPONSIBLE PERSON USAMRMC
a. REPORT	b. ABSTRACT	c. THIS PAGE			
U	U	U	UU	22	19b. TELEPHONE NUMBER *(include area code)*

Table of Contents

PROGRESS REPORT SUMMARY

INTRODUCTION

The goal of this project is to develop an online adaptive treatment technique for prostate cancer treatments. During the first year, we have developed parallel deformable image registration, parallel dose calculation and plan optimization algorithms. During the second year, we have been focusing on improving the robustness of the algorithms and improving online image quality.

STUDIES AND RESULTS: YEAR 2

A. Improving image quality

Image quality of cone beam CT (CBCT) is a major obstacle in clinical implementation of online adaptive treatment. CBCT images lack of contrast, and therefore it is not possible to delineate some of the region-of-interest (ROI). The main reasons for poor image quality are due to excessive scatter and suboptimal detector performance. We have designed a new online imaging system – Tetrahedron Beam Computed Tomography (TBCT) that can conquer these problems[1,2].
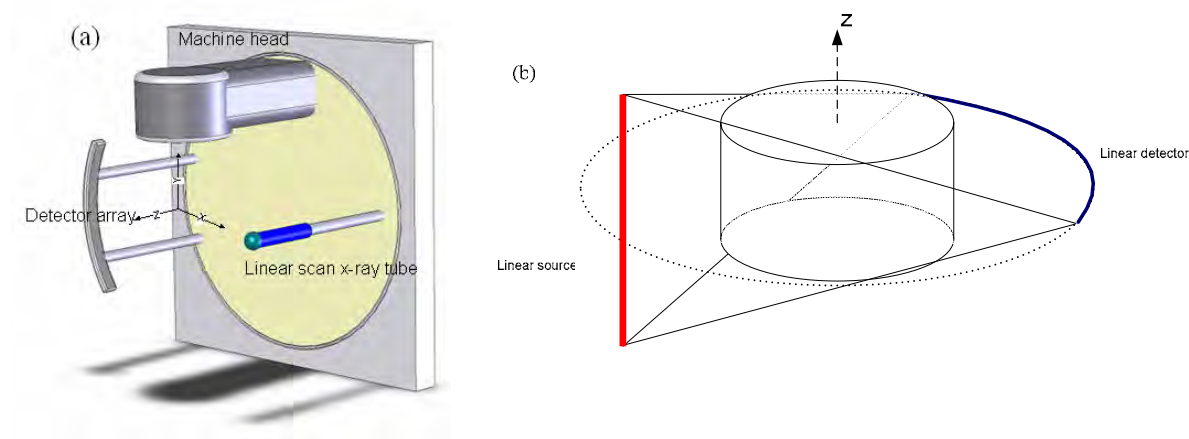

Figure 1 The new system design for online imaging: Tetrahedron Beam Computed Tomography (TBCT): (a) mounted on radiotherapy treatment machine, (b) diagram of scanning geometry.

Figure 1 shows the design of TBCT. This system uses a linear scan x-ray tube and a linear detector array. Due to its unique geometry, the majority of scatter photons are rejected. In addition, it uses the same type of high quality detector as diagnostic CT scanners. Therefore, it is expected to be able to achieve the same image quality as a diagnostic CT scanner. We have acquired an NIH R21 grant to develop a benchtop system. This project was also presented at the 2008 AAPM annual conference. A manuscript has been submitted to Medical Physics Journal, and is currently under review.

B. Development of a fast treatment delivery method

During the first year, we implemented a fast parallel treatment plan optimization method using a Beowulf cluster with a Message Passing Interface. To prepare for clinical implementation, in the second year, we are focusing on accelerating treatment delivery. While online adaptive planning takes care of interfraction motion, the target may also undergo significant intrafraction motion due to patient and bowel movement. It is also noted that intrafraction motion increases with treatment time. This justifies the importance of a faster treatment delivery method.

VMAT is a new dynamic treatment delivery method which can significantly shorten the treatment time. The treatment planning method for VMAT however is not mature. We are developing a robust VMAT treatment planning method which incorporates MLC constraints into the optimization process.

Figure 2 shows the flow chart of our IMAT treatment planning method. It starts with regular sliding window IMRT treatment planning then corrects the rotation angle difference in iterations. One major advantage of this treatment planning method is the robustness. This is a very important feature for online adaptive treatment since a new plan is generated for every treatment.

Figure 3 compares the difference between the IMAT treatment planning method we developed and regular 7 field IMRT treatment planning. We can see the dose distribution from IMAT treatment planning is very similar to regular

Figure 2 Flow chart of IMAT treatment planning based on iterative fluence intensity optimization and sliding window conversion.

IMRT treatment. It is noted that the target dose by IMAT treatment planning is more uniform than IMRT. The overall objective score of IMAT is lower than that from 7 field IMRT (0.0699 vs. 0.0994, respectively). We believe the slight improvement is due to the freedom of selecting optimal angles in IMAT planning. The major improvement in the IMAT method is that it can be delivered within 2-4 minutes, compared to 15 minutes for a regular IMRT treatment.

While primarily developed for prostate online adaptive treatment, the new IMAT treatment planning method shows much broader applications in all treatment sites. Head and neck VMAT treatment planning was difficult because of the difficulty of converting complicated fluences to deliverable MLC leaf sequences. Our new method solves this problem by taking account of MLC constraints during optimization iterations.

Because of the freedom of choosing gantry angles, the IMAT treatment planning is more computationally expensive. This problem can be easily solved by using the parallel dose calculation and optimization algorithms that we have developed previously. Besides that, we are also working on Graphic Processing Unit (GPU)-based parallel computing for dose calculation and optimization. The GPU is a cost effective parallel computing resource. A single GPU may
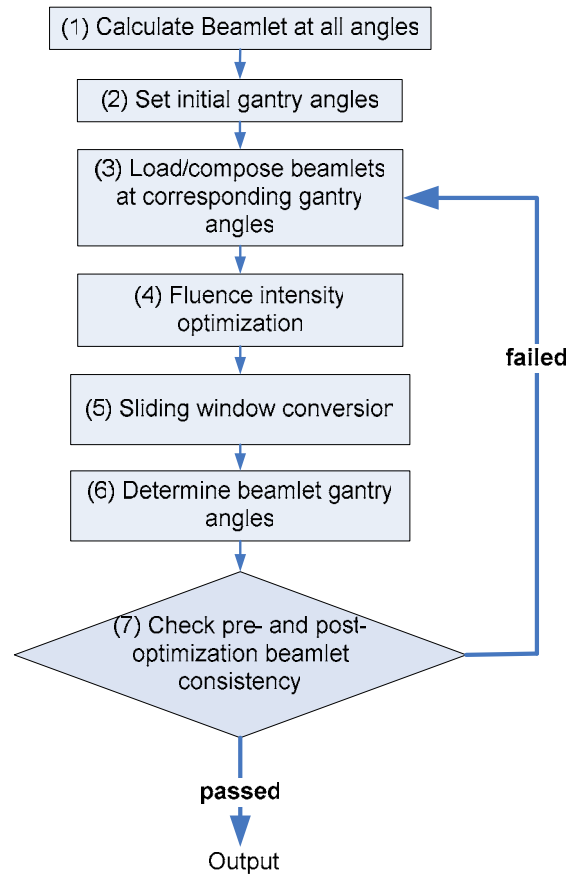
surpass the computing capacity of a medium scale computer cluster. We expect application of the GPU will further boost the speed of computation for dose calculation and optimization.
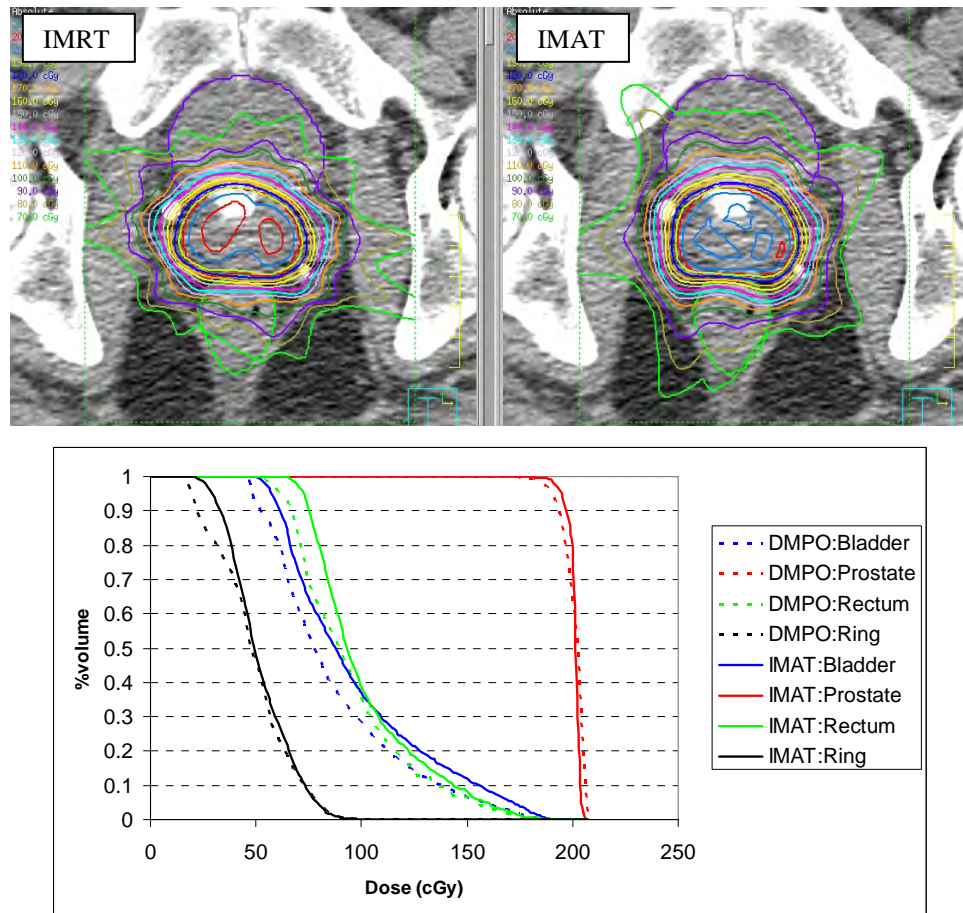

Figure 3 Comparison of IMRT treatment planning (top) and IMAT treatment planning (bottom). The dose distributions and DVHs are very similar, but IMAT treatment can be delivered much faster, so the impact of intrafraction motion will be minimized.

We will submit abstracts to AAPM and ASTRO annual conferences in March 2009 regarding to the IMAT treatment planning method. We also plan to submit the implementation of GPU-based parallel optimization and deformable image registration to AAPM. Manuscripts of publication will be prepared and submitted a few months later.

C. Model-based automatic segmentation of ROI for prostate treatment

Previously, we developed intensity-based deformable image registration algorithms[3,4]. The algorithms have been proven to be very robust in some treatment sites, such as head and neck, breast and lung. However this algorithm is not often successful for organs in the pelvis. This is due to the extremely large deformation of the bladder and large variation of the contents in the rectum.

To solve this problem, we decided to change our plan. We are working on combining the model-based automatic segmentation with intensity based segmentation. We represented the organ using an ROI surface mesh. Figure 4 shows the surface mesh of the rectum. The surface mesh

is created on treatment planning CT images, then distance transformations are performed to calculate the distance of pixels to the boundary. With boundary and distance information, we can treat voxels inside and outside organ differently. We can also weight the voxels basing on its distance to the boundary. So we can emphasize image information closer to the boundary. For the shape change, we are currently using penalties on nodal displacement. When we accumulate enough data, we can perform PCA analysis to determine the eigenspace that organs deform and penalize the deformation that is out of the eigenspace.
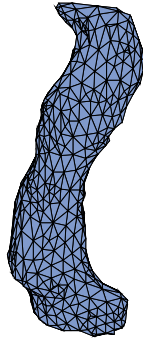

Figure 4 Surface mesh of the rectum. Using the surface representation, we can use distance information to emphasize on voxels closer to the boundary. We are also able to limit the shape change based on statistical model.

KEY RESEACH ACCOMPLISHMENT

1. We have invented a new imaging system which can produce diagnostic quality images online for image guided radiotherapy. We are building a benchtop system with an NIH grant. We expect a clinical prototype system will be built within three years.

2. We have developed an IMAT treatment planning method that significantly shortens treatment delivery time. This method can minimize the impact of intrafraction organ motion during online adaptive treatments. We expect clinical implementation of this treatment planning method within 1-2 years.

3. We are currently combining voxel intensity-based deformable image registration with model based image segmentation. This method may overcome the problems of inconsistent rectum filling and large organ deformation. We expect this method can be fully developed within a few months, after which large scale evaluations will be performed.

REPORTABLE OUTCOMES:

Peer reviewed publications:
1. Tiezhi Zhang, Derek Schulze, Xiaochao Xu, "Tetrahedron Beam CT (TBCT): A New Design of Online Imaging System for Image Guided Radiotherapy", Submitted to Medical Physics Journal.
2. Tiezhi Zhang, Yuwei Chi et al, "Automatic Delineation of Online Head-And-Neck Computed Tomography Images: Toward Online Adaptive Radiotherapy", International Journal of Radiation Oncology, Biology and Physics 2007 68(5): 1572-8.
3. Derek Schulze, Tiezhi Zhang, "Comparison of various online IGRT strategies: The benefits of online treatment plan re-optimization", Radiotherapy and Oncology, in press.

Conference presentations:
1. T. Zhang, D. Schulze, "Tetrahedron Beam CT (TBCT): A New Design of Online Imaging System for IGRT", AAPM annual conference, 2008.
2. D. Schulze, T. Zhang, "Techniques of Online IMRT Plan Re-Optimization for Prostate Cancer Treatments", 50th ASTRO annual conference, Boston, MA, 2008.
3. T. Zhang, *et al, "Online delineation of head and neck CT images",* 49th AAPM annual conference, Minneapolis, MN, 2007
4. T. Zhang, D. Schulze, et al, "Online Adaptive Prostate Cancer Intensity Modulated Radiation Treatment (IMRT): Method of Online Plan Re-optimization" 49th ASTRO annual conference, Los Angels, CA, 2007
5. D. Schulze, T. Zhang, et al, "Dosimetric Comparison of Various Online Adaptive Prostate Cancer Treatment Techniques", Los Angels, CA, 2007
6. *T. Zhang, et al, "Clinical Applications of 3D and 4D Deformable Image Registration for Image Guided Radiotherapy*", 48th AAPM annual conference, Orlando, FL, 2006
7. *T. Zhang, et al, "Automatic Delineation of Daily CT Images for Online Plan Adjustments: Method and Quantitative Validation",* 48th ASTRO annual conference, Philadelphia, PA, 2006
8. *L. Burgess, T. Zhang, et al, "Image Guided Radiotherapy by Online Plan Re-optimization: Studies of Dosimetric Benefits by Treatment Simulations",* 48th ASTRO annual conference, Philadelphia, PA, 2006

Degrees obtained:

1. Derek Schulze, Master of Science, Department of Medical Physics, Wayne State University, Detroit, Michigan

Funding applied for:

1. Development of A Quasi-CBCT System for Image Guided Radiotherapy, PI, Tiezhi Zhang, NIH R21, Started on 3/1/2008
   In this proposal, we will develop a novel imaging system using a linear x-ray source and a linear detector. This imaging system may significantly improve the quality of online images, which is critically important for online ROI delineation.

CONCLUSIONS:

During the second year of this study, we are aiming at future clinical implementation of online adaptive treatment. We have invented a new imaging technique (TBCT) to improve online image quality. We have also developed an IMAT treatment planning method which can shorten the treatment time, thereby minimizing intrafraction motion.

Automatic image segmentation of ROIs for prostate treatment remains a very challenging issue. We are developing a model-based segmentation method which may overcome the existing problems. We expect this method can be developed within a few months. We will perform a large-scale evaluation study thereafter.

REFERENCE:

1. T. Zhang, D. Schulze, "Tetrahedron Beam CT (TBCT): A New Design of Online Imaging System for IGRT", AAPM annual conference, 2008 (Abstract).
2. T. Zhang, Derek Schulze, Xiaochao Xu, *"Tetrahedron Beam CT (TBCT): A New Design of Online Imaging System for Image Guided Radiotherapy"*, Submitted to Medical Physics Journal.

3. T. Zhang, Y Chi *et al,* "Automatic Delineation of Online Head-And-Neck Computed Tomography Images: Toward Online Adaptive Radiotherapy", International Journal of Radiation Oncology, Biology and Physics 2007 68(5): 1572-8.
4. Y Chi, J Liang, T Zhang, *et al,* "Automatic Contour Delineation On Cone Beam CT (CBCT) and Verification", American Association of Physics in Medicine 50th Annual Conference, Huston, TX, 2008 (Abstract).
5. T Zhang, *et al, "Online delineation of head and neck CT images",* 49th AAPM annual conference, Minneapolis, MN, 2007 (Abstract).

AAPM annual conference 2008 abstract:

Title: Tetrahedron Beam CT (TBCT): A New Design of Online Imaging System for IGRT
Authors: Tiezhi Zhang, Derek Schulze

Purpose: Cone-beam computed tomography (CBCT) is an important online imaging modality for image-guided radiotherapy (IGRT) as well as other forms of image guided interventions. However, current CBCT image quality is inferior to that of the diagnostic fan beam CT. We have designed a novel Tetrahedron Beam Computed Tomography (TBCT) imaging system that may achieve the same diagnostic quality as helical CT scanners.

Material and Methods: The TBCT imaging system is comprised of a linear scan x-ray source and a linear discrete x-ray detector array. The axis of linear x-ray tube and the detector array are aligned perpendicular to and within the rotation plane, respectively. The x-ray beams are narrowly collimated into fan beams and focused to the linear detector. Detector and x-ray tube rotate slowly while the fan beams scan quickly along the axis. The TBCT reconstruction geometry is similar to CBCT. Approximate and exact reconstruction algorithms can be modified for TBCT reconstruction.

Results: TBCT will produce diagnostic quality online images due to its scatter rejection mechanism and the use of high-performance discrete x-ray detectors. TBCT also has several other advantages such as larger clearance, ease of performing dynamic field size and mAs controls, etc.

Conclusion: TBCT will significantly improve online image quality. Clinical implementation of TBCT would be of importance in IGRT as well as other forms of image guided interventions.
.

Title: Techniques of Online IMRT Plan Re-optimization for prostate cancer treatments
Authors: Derek Schulze M.S. and Tiezhi Zhang, Ph.D.

Introduction

Online IMRT treatment plan re-optimization can significantly reduce dose to critical organs. The computation speed of current IMRT treatment planning is not fast enough for online re-planning. We have developed several methods which may dramatically expedite dose calculation and optimization and allow for IMRT paln re-optimization online.

Methods & Materials

Pre-treatment planning was performed. The beamlet doses were calculated and stored for daily re-planning. On the treatment day, a 3D image (such as CBCT) of the patient is acquired. Region-of-interests were automatically contoured using our deformable image registration software. Instead of recalculating dose on the daily images, the pre-treatment beamlets were then loaded. Then for each dose voxel, the dose values were corrected for equivalent radiation path length and inverse square distance change in the online images. The accuracy of the corrected dose was validated using a 3D gamma index evaluation. Traditional dose calculations on the online image ("true dose") were used as the standards of accuracy. This corrected beamlet dose was then used to perform the daily optimization. For plan re-optmization, Projection Onto Convex Set (POCS) optimization algorithm was implemented on a multi-node Beowulf cluster using Message Passing Interface (MPI) parallel programming package. The speedup factor of the parallel algorithms was benchmarked. After online re-optimization, the new plan can be used for online adaptive treatment.

Results

Compared to recalculating dose on the online image, correction of pre-treatment beamlet approach is fast and does not require accurate calibration of CT number which is difficult to achieve on cone beam CT. Although approximate, the corrected dose is very close to the exact dose calculation method. Benchmark results showed that the parallel optimization algorithm is highly scalable. According to Amdahl's Law , the serial component of the algorithm is only about 2.6%. Based on the result, it is predicated that a computer cluster with 32-core CPU could complete the online prostate IMRT optimization within 17 seconds.

Conclusion

Online re-optimization of prostate cancer treatments is made possible with the presented techniques.The computation time required for treatment plan optimization is sufficiently reduced by our methods to make the process feasible in an online setting.

Title: Online Region-of-Interest Delineation of Daily Head and Neck Images

Authors; Tiezhi Zhang, Yuwei Chi, Douglas Drake, Di Yan and Elisa Meldolesi

Purpose: Online imaging modalities, such as cone beam computed tomography (CBCT) or CT on-rail provide online volumetric images. A fast, automatic and robust region-of-interest (ROI) delineation method is highly desired in image guided radiation therapy (IGRT). We have developed such a method and tested it via segmentation of head and neck (HN) fan beam CT and CBCT images.

Material and Methods: ROIs on planning CT images were manually delineated using commercial treatment planning system. A variational-based deformable image registration algorithm was implemented to register planning CT images to daily CT images. ROIs on planning CT images were automatically mapped to daily images using voxel matching information between planning and daily image datasets. The results were quantitatively and qualitatively validated by comparing to manual delineation. In order to accelerate computing speed, we paralleled the algorithm using message passing interface (MPI) on a Beowulf cluster with 16 processing elements (PE). Speed improvement was benchmarked.

Results: The discrepancies between automatically and manually delineated ROIs on fan beam images were mostly within 2mm. Automatic segmentation of CBCT images was acceptable by visual inspection. Benchmark results showed that paralleling efficiencies were above 95% and speedup factors were approximately equal to the number of PE used. With 16 PEs online delineation of HN images took about 1 minute.

Conclusion: The online ROI delineation method we have developed is robust, fast and is suitable for HN online adaptive radiation treatments.

Original article

Comparison of various online IGRT strategies: The benefits of online treatment plan re-optimization

Derek Schulze [a,b], Jian Liang [a], Di Yan [a], Tiezhi Zhang [a,*]

[a] Department of Radiation Oncology, William Beaumont Hospital, Royal Oak, MI, USA
[b] Department of Medical Physics, Wayne State University, Detroit, MI, USA

ABSTRACT

Purpose: To compare the dosimetric differences of various online IGRT strategies and to predict potential benefits of online re-optimization techniques in prostate cancer radiation treatments.
Materials and methods: Nine prostate patients were recruited in this study. Each patient has one treatment planning CT images and 10-treatment day CT images. Five different online IGRT strategies were evaluated which include 3D conformal with bone alignment, 3D conformal re-planning via aperture changes, intensity modulated radiation treatment (IMRT) with bone alignment, IMRT with target alignment and IMRT daily re-optimization. Treatment planning and virtual treatment delivery were performed. The delivered doses were obtained using in-house deformable dose mapping software. The results were analyzed using equivalent uniform dose (EUD).
Results: With the same margin, rectum and bladder doses in IMRT plans were about 10% and 5% less than those in CRT plans, respectively. Rectum and bladder doses were reduced as much as 20% if motion margin is reduced by 1 cm. IMRT is more sensitive to organ motion. Large discrepancies of bladder and rectum doses were observed compared to the actual delivered dose with treatment plan predication. The therapeutic ratio can be improved by 14% and 25% for rectum and bladder, respectively, if IMRT online re-planning is employed compared to the IMRT bone alignment approach. The improvement of target alignment approach is similar with 11% and 21% dose reduction to rectum and bladder, respectively. However, underdosing in seminal vesicles was observed on certain patients.
Conclusions: Online treatment plan re-optimization may significantly improve therapeutic ratio in prostate cancer treatments mostly due to the reduction of PTV margin. However, for low risk patient with only prostate involved, online target alignment IMRT treatment would achieve similar results as online re-planning. For all IGRT approaches, the delivered organ-at-risk doses may be significantly different from treatment planning prediction.

© 2008 Elsevier Ireland Ltd. All rights reserved.

The purpose of treatment-room imaging technologies has been to accurately position the patient for daily treatments. This increased accuracy justifies a smaller clinical target volume to planning target volume (CTV–PTV) margin [1], decreasing the consequent collateral damage to normal tissues. While treatment-room imaging methods are certainly a step forward for radiation oncology, the efficacy of these image-guided treatments depends on a treatment plan optimized using a single snapshot of the patient anatomy, typically via the simulation computed tomography (CT). This planning method assumes that the shape and position of the target do not change from day to day. This assumption is often violated due to setup variation and daily anatomic position changes. As image guidance technologies begin to provide a new level of information during each treatment, new strategies should be adopted to ensure that the best treatments are delivered to the greatest number of patients.

Perhaps the key issue in image guidance is how the information is used to modify treatment [2,3]. We classify the online image-guided radiation treatments (IGRT) into three different precision levels: (1) *bony alignment*, (2) *target alignment*, and (3) *re-planning*.

Bony alignment. Of the three IGRT strategies, bony alignment has the lowest requirement for online image quality, as projection radiographic image quality allows visibility of high contrast bony landmarks but not soft tissues. This method can be implemented by using electronic portal imaging devices (EPIDs) [4]. In clinical treatment, the 2D megavoltage (MV) images can be registered to a digitally reconstructed radiograph (DRR) or to treatment planning CT via 2D–3D registration [5]. Depending on the definition of registration volume and image quality, volumetric online images from kilovoltage cone beam CT (kV-CBCT) and MV-CBCT may also

be registered at bony structures due to the high contrast to surrounding soft tissues [6]. Most current IGRT treatments correct only the three translational components of rigid-body motion. Six-degree-of-freedom corrections can be achieved with a robotic couch (Hexpod™, Medical Intelligence GmbH, Schwabmünchen, Germany) [7] or by rotating the couch, collimator and gantry altogether [8]. In the treatment simulation study, we registered the daily treatment images to the planning CT images at the pelvic bones with six degrees of freedom to simulate bony alignment approach.

Target alignment. Aligning directly to the target requires better image quality. The boundary of the low contrast (soft tissue) treatment target needs to be identified. For prostate treatments in particular, it may be difficult to align the target in IGRT treatment using CBCT due to its inferior image quality. Another approach to align at the target is to use implanted fiducial markers, which are visible through portal imaging [9]. The basic application of this technology would be to identify the target center-of-mass based on the average position of three markers. In our clinical experience, however, we found that the target motion may include large rotational components. It is unrealistic to fully correct the rotation [10]. Thus, in the simulation study, we only correct the translation component by translating to the center-of-mass.

Re-planning. If the target and organs-at-risk (OARs) can be delineated on online volumetric images, it is possible to generate a new plan in each treatment day [11]. For 3D conformal radiation treatment (3D-CRT) plans, the beam aperture can be changed according to the shape of the target seen in the beam's-eye-view (BEV) [12]. For intensity modulated radiation therapy (IMRT) plans, the beamlet weight can be re-optimized on a daily basis to minimize the dose to the OAR while maintaining the target dose [13,14]. It is reasonable to use rectum and bladder walls during inverse planning of prostate cancer treatments, so long as the intrafraction motion can be limited to a negligible level. With these biologically relevant inverse planning objectives, the dose to the OAR may possibly be further reduced.

Re-planning theoretically provides the highest precision and does not need specialized hardware such as the robotic couch. However, online re-planning requires superior online image quality, as well as fast and robust algorithms to perform automatic region-of-interest (ROI) delineation [15], dose calculation, and beamlet weight optimization. We are actively developing the techniques to facilitate online re-planning. In this study, we performed both 3D-CRT and IMRT treatment planning and treatment simulation studies for several online IGRT strategies. The purpose of this study is to investigate the potential benefits of the *re-planning* approach in prostate cancer treatments, and to characterize the limits of the other IGRT methods.

Methods and materials

Treatment planning

Image data from nine prostate cancer patients treated at William Beaumont Hospital in Royal Oak, MI, USA, were used in this study. The nine patients were randomly selected from our patient database. We assume the magnitude of organ motions of these randomly selected patients represent typical prostate population. Treatment planning CT images were acquired with a conventional helical CT scanner. There was no bowel preparatory instruction or procedure for any simulation or treatment day images. For each of these images, contours of prostate, seminal vesicles (SV), rectum (volume and wall), and bladder (volume and wall) were hand-drawn by a single observer. Based upon the contours, treatment plans were generated using the Pinnacle™ treatment planning system (TPS) (Philips Radiation Oncology System, Madison, WI). The patients were planned as if they had intermediate or high risk disease, and therefore the CTV included both prostate and seminal vesicles. The average prostate volume was 40.7 cm^3 (range: 22.5–54.4 cm^3). OARs were limited to bladder and rectum. The average rectum volume was 120.5 cm^3 (range: 45.0–189.5 cm^3).

The prostate shows significant movement relative to the pelvic bones [16]. Thus, a uniform 1-cm CTV–PTV margin is used to compensate for interfraction organ motion in both 3D-CRT and IMRT treatment plans which are intended for use with the bony alignment treatment method. Results from these treatments will demonstrate the adequacy of a widely practiced IGRT method.

Since the target alignment treatment method can account for translational interfraction motion, the motion margin can be greatly reduced. In the 3D-CRT re-planning and IMRT re-planning methods, all interfraction motions are expected to be compensated, and so there is no motion margin component in the PTV for these methods. This will also give us a feeling about the dosimetric robustness of various IGRT methods to the target translations, deformations, and to the rotations involved. Intrafraction motion is neglected in this study.

An arbitrary dose of 91.0 Gy was prescribed to the PTV, though results will focus on relative dose values, scalable to any prescription. All treatment plans used five coplanar beams at 0°, 81°, 144°, 216°, and 279°. DVH-based dose–volume objectives were chosen to minimize bladder and rectum doses while maintaining PTV dose uniformity during inverse planning.

The IGRT approaches and the corresponding treatment planning methods are listed in Table 1. Five 3D-CRT and IMRT treatment planning methods formed the bases for the online IGRT treatments:

(1) *CRT 1-cm.* 3D-conformal radiotherapy to 95% of the isocenter with 1-cm CTV-to-PTV margin and 6-mm PTV-to-block penumbra. This plan was used for CRT bony alignment IGRT approach (*CRT Bone*).

(2) *CRT 0-cm.* 3D-CRT plan to 95% of the isocenter with 0-cm CTV-to-PTV margin and 6-mm PTV-to-block penumbra. This plan was used for CRT re-planning via aperture change approach (*CRT Re-plan*).

(3) *IMRT 1-cm.* Inverse-planned IMRT with 1-cm CTV-to-PTV margins and OAR-volume as optimization objectives. This was used for IMRT bone alignment treatments (*IMRT Bone*).

(4) *IMRT 0-cm volume.* Inverse-planned IMRT with 0-cm CTV-to-PTV margins and OAR volumes as objectives. This method

Table 1
A summary of IGRT approaches simulated in this study

Planning method	CTV–PTV margin (cm)	Organs-at-risk	Image guidance	Treatment name
CRT 1-cm	1	n/a	Bony Alignment	CRT Bone
CRT 0-cm	0	n/a	Block shaped to daily PTV	CRT Re-plan
IMRT 1-cm	1	Bladder and rectum volumes	Bony Alignment	IMRT Bone
IMRT 0-cm Volume	0	Bladder and rectum volumes	Isocenter shifted to daily PTV center-of-mass	IMRT Target
IMRT 0-cm Volume	0	Bladder and rectum volumes	Complete daily IMRT re-optimization	IMRT Re-plan Volume
IMRT 0-cm Wall	0	Bladder and rectum walls	Complete daily IMRT re-optimization	IMRT Re-plan Wall

The information of a row from left to right describes how a planning method relates to an IGRT treatment method.

was used for both IMRT target alignment (*IMRT Target*) and IMRT re-planning with OAR volumes as constraints approach (*IMRT Volume*).

(5) *IMRT 0-cm wall.* Inverse-planned IMRT with 0-cm CTV-to-PTV margins and OAR walls in optimization objectives. This method was used for IMRT re-planning with OAR walls as constraints approach (*IMRT Wall*).

Virtual treatment simulations

In addition to treatment planning CT images, 10-treatment-day helical CTs were also acquired for each patient. The treatment-day images were acquired during the 6–8-week treatment courses with intervals of 3–5 days. The 10-treatment-day images were used to simulate 10 treatment fractions for all online IGRT techniques. The daily images were registered to the planning image using bony anatomy in Pinnacle. The ROIs were manually delineated on all daily images after bony registration. As an indication of the range of interfraction motion, Fig. 1 shows a treatment planning image with contours overlaid from bone registered daily images.

Ideally, treating a patient positioned by bony landmarks can be simulated by calculating dose on the daily images. However, due to technical issues with Pinnacle, dose calculation on daily images was not possible for the images where non-zero rotational components exist in registration parameters. Previous studies have shown that replacing a daily CT with the planning CT introduces minimal dose calculation error [17]. By using daily images which were registered to the planning image without rotation, we were able to determine that calculating daily dose on the planning image introduces an EUD error in the studied ROIs of less than 1%. Thus in this study, daily treatment dose was calculated using voxel densities from the planning CT, as this method introduces negligible error. Calculating DVHs from dose to daily contours will accurately represent all daily motions, as the rotation present in registered daily images will be preserved in the contour shape.

Retrospective virtual treatment simulations were performed in order to compare different online IGRT treatment methods. Compared to interfraction motion, intrafraction motion is relatively small [16]. In this study, we only focused on interfraction motion,

Fig. 1. Planning CT showing bladder (yellow), CTV (red), and rectum (green) contours. Thick lines define contours from the planning day. Thin lines show the positions of the organs on different treatment days. Contours were generated after registration of bony anatomy.

while intrafraction motion was neglected. Treatment methods were simulated that were associated with different levels of image guidance. The relationship between planning methods and treatment methods is summarized in Table 1.

Bony alignment. Bony alignment was simulated by registering the daily treatment images to the planning CT images at the pelvic bones with six degrees of freedom. Doses for *CRT Bone* and *IMRT Bone* treatments were calculated using the unmodified *CRT 1-cm* and *IMRT 1-cm* plans. This simulates the position correction available from standard imaging systems combined with the robotic couch.

Target alignment. Aligning directly to the target requires better image quality. The boundary of the low contrast (soft tissue) treatment target needs to be identified. For prostate treatments in particular, it may be difficult to align the target in IGRT treatment using CBCT due to its inferior image quality. Another approach is to use a portal imager to visualize implanted fiducial markers [9]. One application of this technology that is possible with CBCT would be to identify the target based on the average 3D position of three markers. In our clinical experience, however, we found that the target motion may include large rotational components. With the standard couch, it is unrealistic to correct the rotation without modifying the treatment plan. Furthermore, the maximum rotation of the Hexpod™ robotic couch is about 2.5–3.0°, and so some large rotations cannot be corrected in this fashion. In this study, we simulated an image-guided treatment available to many institutions by only translating the isocenter to the daily target's center-of-mass. After moving the isocenter, daily doses were calculated using the original *IMRT 0 cm Volume* plans. This approximates the use of implanted markers based upon the assumption that marker position accurately reflects target position. For the purposes of this study, this treatment method was labeled *IMRT Target*.

Re-planning. The *CRT Re-plan* treatments started from the *CRT 0-cm* plan. On each treatment day, beam apertures were changed to the daily shape of the target in the beam's-eye-view (BEV) [12], but the monitor units (MUs) delivered by each beam were kept the same as in the original treatment plan. This makes the re-planning process much simpler from a computational standpoint, as dose re-calculation is unnecessary.

For intensity modulated radiation therapy (IMRT) plans, the beamlet weight can be re-optimized on a daily basis to minimize the dose to the OAR while maintaining the target dose [14]. So long as the intrafraction motion can be limited to a negligible level, it is reasonable to use rectum and bladder walls during inverse planning of prostate cancer treatments. With these biologically relevant inverse planning objectives, the dose to the OAR may possibly be further reduced.

The *IMRT Re-plan Volume* and *IMRT Re-plan Wall* treatments involve complete re-planning on each treatment day. Moving beyond the *CRT Re-plan* method to these treatments requires overcoming the technical challenges of online dose calculation and beamlet weight optimization. To simulate this process, daily doses were calculated after daily re-planning using the *IMRT 0-cm Volume* and *IMRT 0-cm Wall* planning methods.

Dose accumulation

All daily doses were exported to an in-house dose accumulation software utility [18]. In this utility, a finite element (FE)-based deformable registration algorithm was used to obtain voxel matching information between daily and planning CT images. FE models were created using ROI contours from planning CT images. The daily contours were used as boundary conditions to limit the organ deformation. The deformation state with minimum internal elastic energy was obtained. The voxel displacements were obtained by interpolating the FE results to the CT voxel grid.
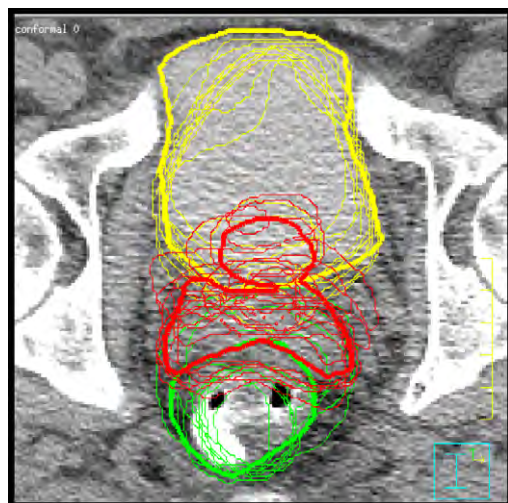
With voxel displacements, dose accumulation is straightforward. The accumulated dose D at position $\vec{x}$, can be obtained by

$$D(\vec{x}) = \sum_{j=1}^{N} d_j(\vec{x} + \vec{u}), \qquad (1)$$

where N is the total number of fractions, d_j the daily dose from the treatment fraction j, and $\vec{u}$ is the daily displacement of the FE sub-volume from its original position $\vec{x}$.

Evaluation methods

Dose from treatment planning and simulated delivery was evaluated using the equivalent uniform dose (EUD), as in Eq. (2), where V is the reference volume, and $D(v)$ is the dose to the sub-volume v.

$$EUD(V, a) = \left(\sum_{v \in V} \frac{v}{V} \cdot D^a(v) \right)^{1/a} \qquad (2)$$

As in the previous studies [19], the volume parameter for prostate and seminal vesicles was chosen as $a = -7$. With regard to normal tissues, values were chosen as $a = 2$ for bladder, and $a = 8.33$ for rectum.

Results

Comparisons of treatment planning results

This study included five different treatment planning methods. 3D-CRT and IMRT were used in treatment planning, and different treatment planning methods used different CTV–PTV margins (0-cm and 1-cm). The EUDs of the OARs (rectum and bladder) were calculated and compared to the prostate EUD. Unless otherwise noted, percentage values discussed in the following treatment re-

sults are based upon the target (prostate) EUD dose in the respective treatment plan.

In order to provide a complete description of results from one randomly selected patient, Fig. 2 shows the dose-volume histograms (DVHs) of one patient (#9) from the five planning methods studied. It can be seen that IMRT plans have less homogeneous target dose. Bladder dose appears to be similar for both plans with 1 cm margins. IMRT significantly reduces rectum dose. Rectum dose is similar between the *CRT* 0-cm method and the *IMRT* 1-cm method, even though the latter one has a 1-cm interfraction margin.

The planned bladder and rectum EUDs for all patients are summarized in Table 2. For the same patient, OAR doses by all treatment planning methods were also normalized to the *IMRT* 1-cm plan. When rectum and bladder walls were used in IMRT optimization, the shapes of the dose distributions look different as compared to using the volumes. The top panels of Fig. 3 show the fluence maps of the anterior–posterior (AP) beam and isodose distributions from *IMRT* 0-cm *Volume* and *IMRT* 0-cm *Wall* plans. In the volume-based plan, fluence is decreasing where the beam passes a greater distance through the whole organ, while intensity in the wall-based plan is decreased only in a ring where pathlength through the bladder wall is greater. The isodose lines form a "W" shape as they first retract along the walls, then extend into the center of bladder and rectum in *IMRT Wall* plan. On the contrary, the *IMRT Volume* plan has lower weightings for the beamlets through the center of the bladder, with isodose lines extending a minimum distance into any part of the sensitive organs. Despite this obvious qualitative difference, the improvement of the bladder and rectum EUD dose (as a percent of prostate dose) from *IMRT Volume* to *IMRT Wall* plans is barely noticeable at $1.01 \pm 0.97\%$ and $1.71 \pm 1.53\%$, respectively.

Selecting an altogether different planning method has a greater impact on the OAR dose than changing the particular definition of the normal tissue volume. With the same 0-cm margin, IMRT plans
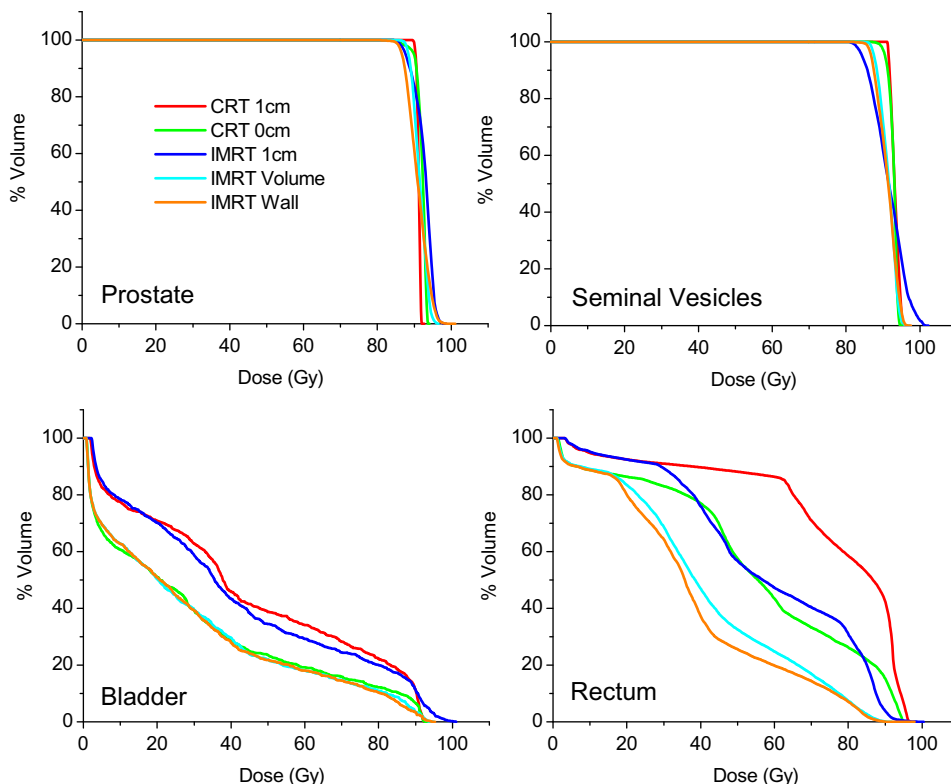

Fig. 2. Comparison of dose from five treatment planning methods for patient #9, described by dose-volume histograms.

Table 2
Comparison of planned rectum and bladder EUD doses from various treatment planning methods

Patient #	CRT 1-cm (%)	CRT 0-cm (%)	IMRT 1-cm (%)	IMRT volume (%)	IMRT wall (%)
Rectum					
1	95.0	84.3	82.3	67.8	66.7
2	88.9	82.5	85.9	74.4	75.4
3	88.5	80.5	88.1	74.1	70.2
4	92.5	84.6	82.9	77.4	74.2
5	89.9	80.3	82.1	72.6	70.7
6	93.6	83.6	83.3	70.7	70.1
7	89.4	77.9	85.2	70.2	68.4
8	92.3	80.1	85.7	71.1	68.0
9	94.7	84.6	82.8	72.0	71.2
Mean	91.6	82.1	84.3	72.3	70.5
Bladder					
1	78.6	63.6	67.7	56.2	54.0
2	76.2	59.6	67.3	52.4	52.8
3	50.9	40.1	52.5	40.8	39.7
4	63.3	49.4	58.1	48.1	48.3
5	70.5	53.0	64.7	51.6	50.3
6	83.5	66.8	73.2	59.5	57.4
7	60.8	47.3	58.7	47.5	45.8
8	64.9	48.3	60.0	46.9	45.7
9	59.3	45.9	56.4	45.0	44.9
Mean	67.6	52.7	62.1	49.8	48.8

The values are expressed as percentages of target (prostate) EUD dose.

(*IMRT Volume* and *IMRT Wall*) reduced bladder dose by an average of only 3% compared to 3D-CRT plans (CRT-0-cm), and rectum doses were reduced by 11%. When using a 1-cm margin, there are decreases when changing from CRT to IMRT plans in rectum and bladder doses, by about 7% and 6% of target dose, respectively. The choice of an appropriate CTV–PTV margin is a more important factor that determines OAR doses. For the same planning method, the rectum dose in 0-cm margin plans is, respectively, 10% and 11% lower using CRT and IMRT methods than their corresponding plans with 1-cm margins. The bladder dose reductions are even larger, at 15% and 14% when a 0-cm margin is used instead of a 1-cm margin for CRT and IMRT, respectively.

Virtual treatment simulation results

Fractional dose

The fractional doses for different online IGRT strategies were calculated using the methods described in previous sections. Histograms of differences of the individual fraction dose from the planned EUD can be seen in Fig. 4 for all treatment fractions ($N = 90$). All IGRT strategies were able to deliver consistent dose to the prostate. However, dose to the seminal vesicles (as a fraction of planned seminal vesicle dose) was reduced by more than 20% in one fraction from the *IMRT Target* method. On this day, the prostate had moved 0.17 cm to the posterior from the planning position while the seminal vesicles had moved 1.35 cm in the anterior
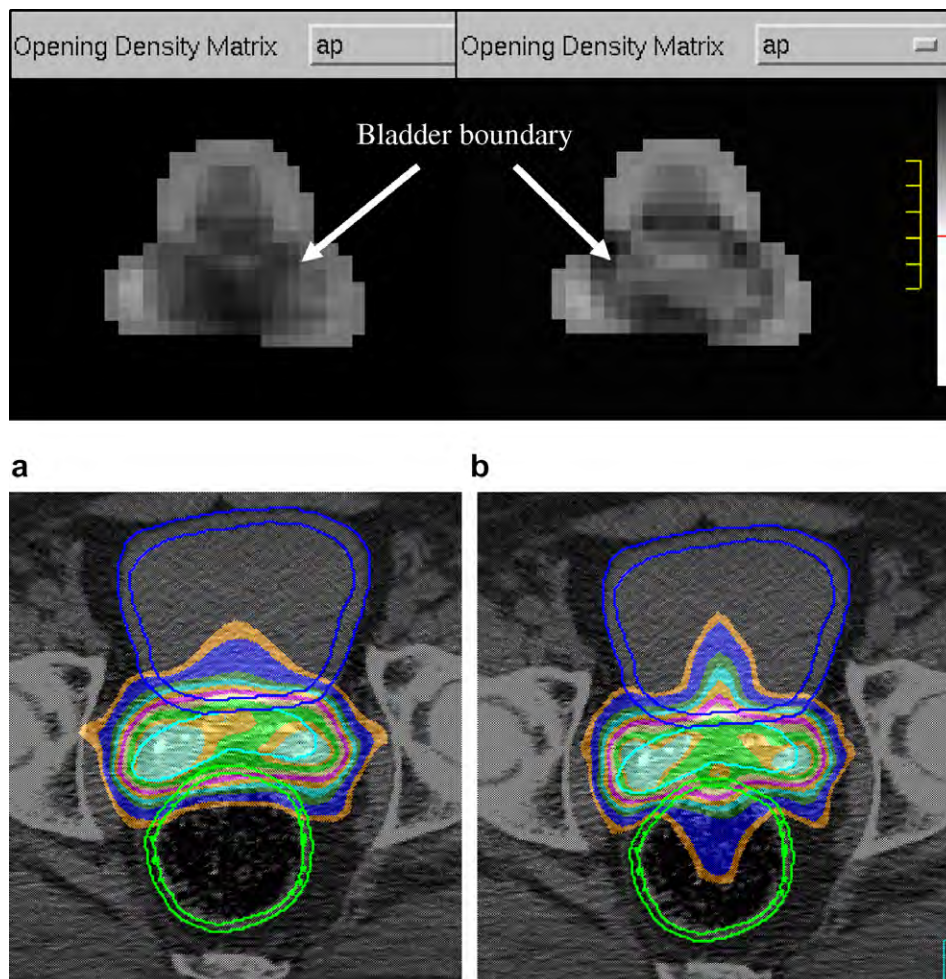

Fig. 3. Top: AP beam fluences from treatment plans optimized with OAR volume (left) and OAR wall (right). Bottom: Isodose profiles from IMRT treatment plans using (a) organ volumes and (b) organ walls. Bladder wall, seminal vesicles, and rectum wall are contoured in dark blue, light blue, and green, respectively. Isodose levels range from 55% to 105% of the isocenter dose.
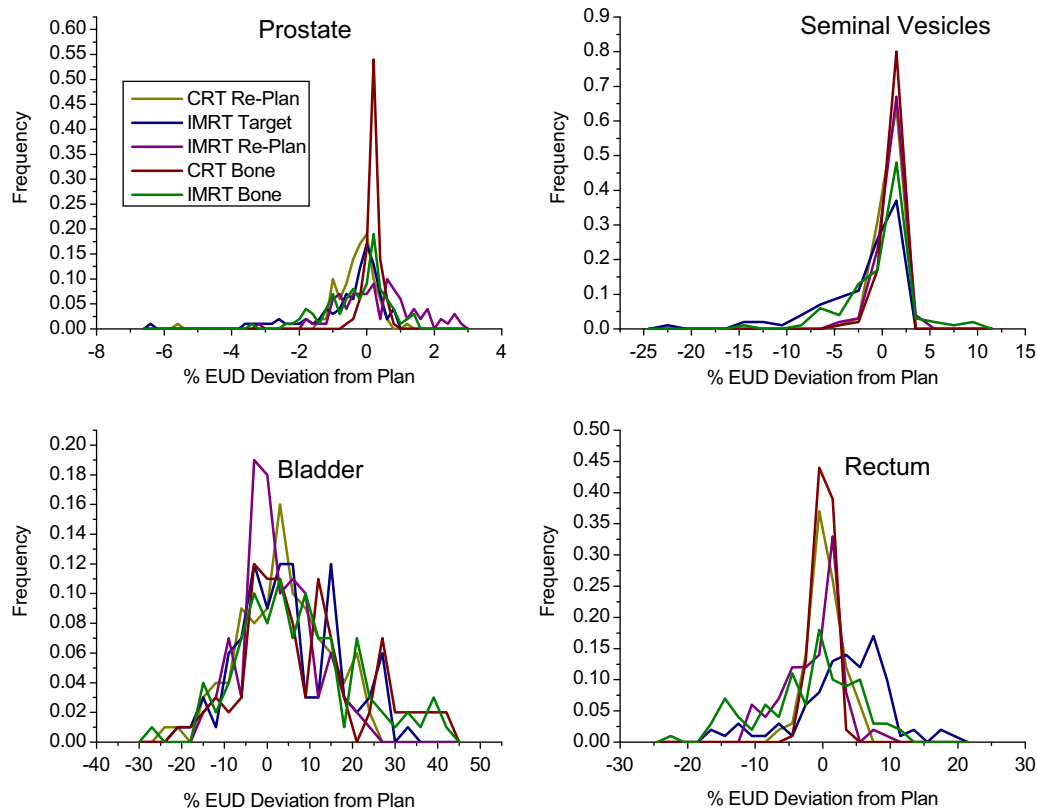
Fig. 4. Histogram of individual fraction deviations from planned EUD, expressed as percent of the respective organ planning dose. Total number of treatment fraction *N* is 90.

direction. There were several fractions where *IMRT Bone* delivered a seminal vesicle dose that was at least 5% less than planned. Blad-

der dose deviation appears to be similarly random for all treatment methods. In the rectum, only the two 3D-CRT methods delivered
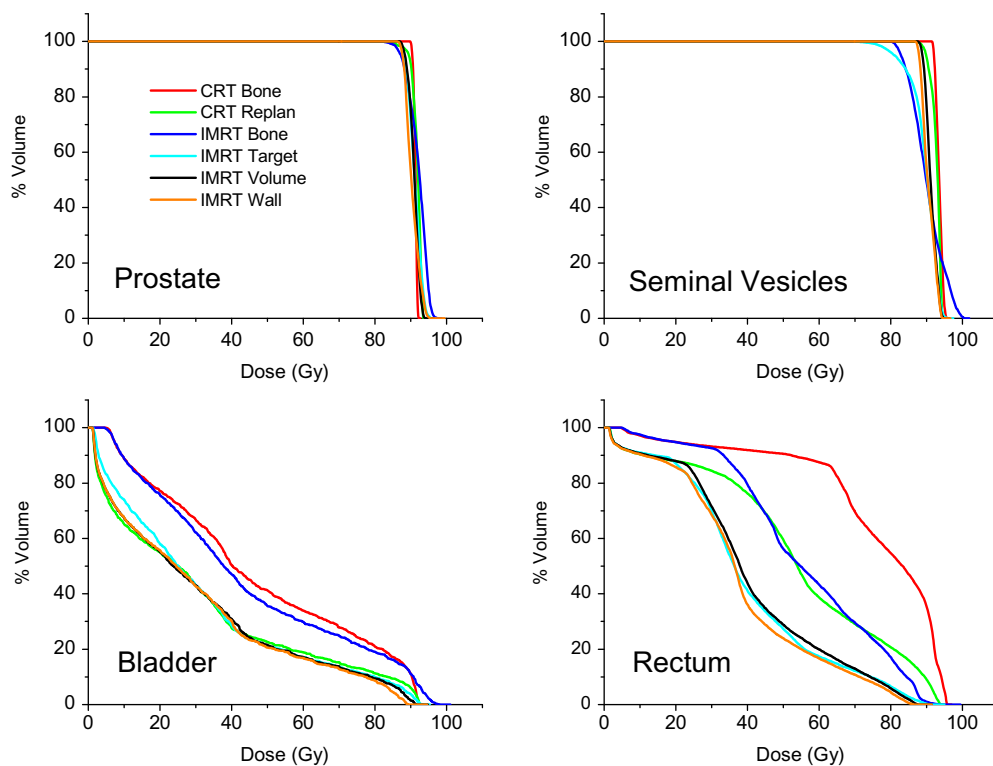

Fig. 5. DVH of accumulated dose after 10 treatment fractions (patient #9).

dose that was consistently within ±10% of the planned amount. Despite this benefit in treatment consistency, CRT plans resulted in larger rectum dose than IMRT plans with the same margin.

Accumulated dose

The fractional doses were accumulated using in-house FE-based dose accumulation software. Fig. 5 shows the DVH of accumulated dose for Patient #9. Fig. 6 shows the accumulated doses for all patients after ten fractions. The EUD values were normalized to the target (prostate) EUD in the treatment plan of the same patient with the same IGRT strategy. The prostates were all well covered, with only one patient's EUD value at about 97% in the IMRT target alignment approach. Seminal vesicles, however, showed a larger difference, with the IMRT target alignment approach showing more severe underdose than other methods. The delivered EUD was only about 93% of the planned value on patient #2. Even with 1-cm CTV–PTV margin, the IMRT bone alignment showed slight underdose on patients #2 and #9. The accumulated dose results support the conclusion derived from individual fraction doses that IMRT is more sensitive to organ motion than 3D-CRT treatments.

Table 3 summarizes rectum and bladder doses achieved by different online IGRT approaches. Remarkable differences in OAR doses are observed when choosing different online IGRT strategies.

The *CRT Bone* approach delivered the highest OAR doses, with the bladder and rectum, respectively, on the average receiving 91% and 71% of target dose. IMRT re-planning approaches obtained the lowest bladder and rectum doses, with average values of 68–69% of target dose to rectum and 49–50% to the bladder. The IMRT target alignment approach obtained OAR doses that are similar to though slightly (1–5%) higher than the IMRT re-planning approaches on most patients. It should be noted that even though the IMRT target alignment method results in similarly low OAR dose, it did not deliver as reliable seminal vesicle dose as re-planning approaches. However, if only the prostate is the target, the IMRT target alignment method would be closer to the re-planning approach.

Difference from treatment plan prediction

A major purpose of treatment planning is to predict OAR doses. With an estimate of the risk of complication based on this dose, an appropriate maximum prescription dose can be determined. However, due to the organ motion, the actual delivered dose may be very different from the prediction in the treatment plan. We plotted the discrepancies between treatment plan prediction and accumulated dose after virtually simulated delivery in Fig. 7. For all IGRT approaches, the deviation of prostate dose is small. Online
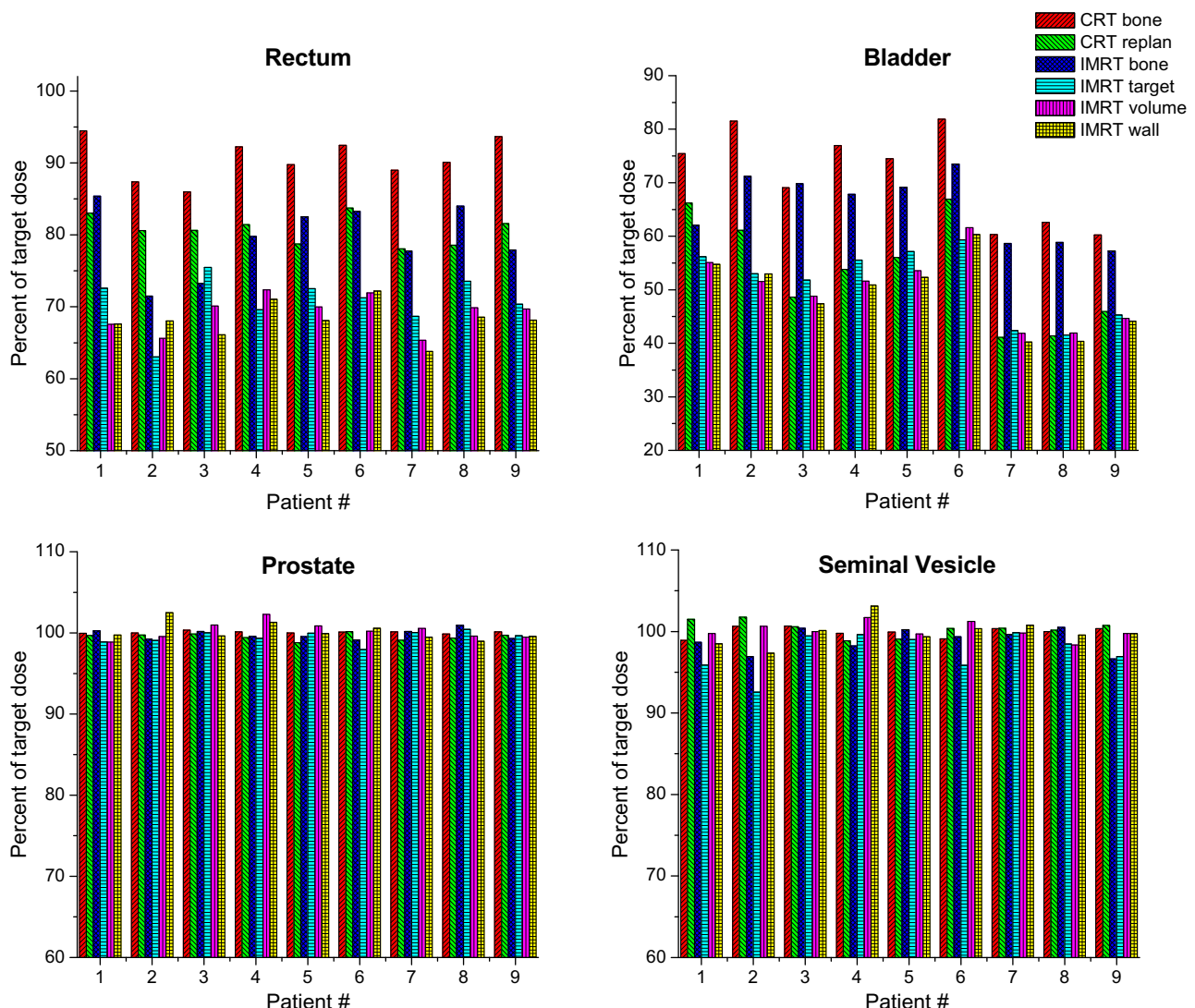

Fig. 6. Accumulated EUD from 10 treatment fractions for different online IGRT strategies.

Table 3
Comparison of delivered rectum and bladder doses by different online IGRT methods

Patient #	CRT bone (%)	CRT re-plan (%)	IMRT bone (%)	IMRT target (%)	IMRT re-plan volume (%)	IMRT re-plan wall (%)
Rectum						
1	94.5	83.3	85.2	73.4	68.3	67.8
2	87.4	80.8	72.0	63.6	65.9	66.4
3	85.7	80.8	73.1	75.4	69.4	66.3
4	92.1	81.9	80.2	70.1	70.7	70.1
5	89.8	79.7	82.9	72.6	69.4	68.2
6	92.4	83.6	84.0	72.7	71.8	71.8
7	88.9	78.8	77.6	68.6	65.0	64.2
8	90.2	79.1	83.2	73.3	70.1	69.3
9	93.5	81.8	78.4	70.6	70.1	68.4
Mean	90.5	81.1	79.6	71.1	69.0	68.0
Bladder						
1	75.5	66.4	61.9	56.8	55.7	54.9
2	81.5	61.3	71.8	53.5	51.8	51.7
3	68.9	48.7	69.7	51.8	48.3	47.6
4	76.9	54.1	68.1	55.9	50.5	50.3
5	74.5	56.7	69.5	57.2	53.1	52.4
6	81.8	66.8	74.1	60.6	61.5	60.0
7	60.3	41.5	58.6	42.4	41.7	40.5
8	62.7	41.7	58.3	41.4	42.1	40.8
9	60.2	46.0	57.7	45.5	44.9	44.3
Mean	71.3	53.7	65.5	51.7	49.9	49.2

The values are expressed as percentages of target (prostate) dose.

IMRT re-planning approaches show small but noticeable target dose variations. This is due to the daily geometry changes that altered the weightings of optimization components. Thus, it may be

necessary to re-scale the monitor units (MUs) based on the prostate dose in daily re-optimization. The seminal vesicles show large variations from IMRT bone and target localization approaches.

The rectum doses show large plan-delivery discrepancies in all IMRT treatments. Although the mean discrepancy across all patients is close to zero, the standard deviation is larger than 5%. The standard deviation is slightly smaller in IMRT re-planning approaches, but not very significant. The 3D-CRT treatments are more consistent, as the mean of discrepancies is close to zero and standard deviation is smaller than 3%. For bladder, all online IGRT approaches show large variations from treatment plan predictions. The standard deviation of plan-delivery discrepancies for this organ is large, around 15% in most IGRT approaches, while the standard deviations for IMRT re-planning approaches are smaller, at about 10%.

Discussion

Traditional radiation treatments strategically treat volumes greater than the clinical target tissues to the prescription dose in order to achieve a high probability of treatment success in spite of daily tumor position uncertainty. Many studies have been done to typify organ motion, and a number of CTV-to-PTV margin recipes [20,21] have been devised to make the selection of margin size a more informed decision. Schaly [2] found that normal tissue dose is not reduced with image guidance alone, but by with the combination of image guidance with smaller CTV–PTV margins. This result is supported by our study.

Interfraction motion has been recognized as the largest contributor to target position uncertainty in tumors unaffected by respira-
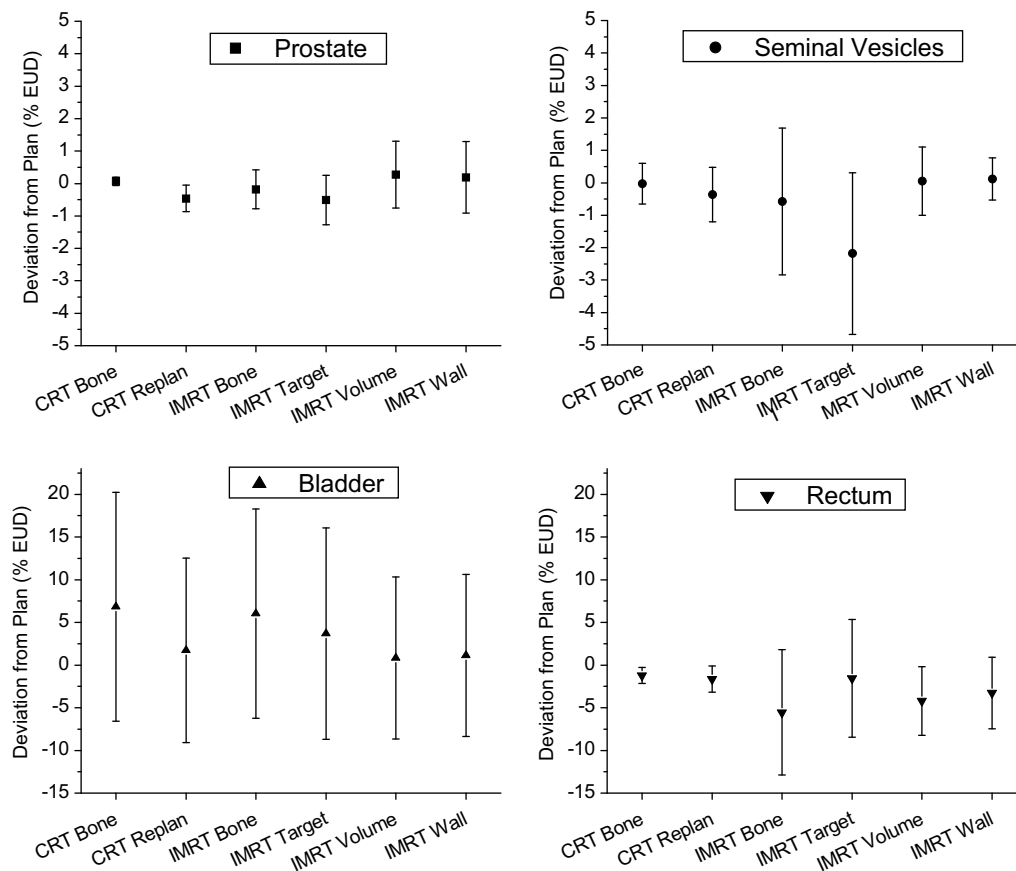

Fig. 7. Discrepancies of cumulative delivered doses from treatment plan prediction, expressed as mean and standard deviation of all patients. The columns are the mean and the error bars are the standard deviation of the difference.

tory motion [16]. In this study, intrafraction motion was not simulated. Ghilezan et al. showed that prostate intrafraction motion correlated with rectal filling [19] and the amplitude of motion increased with elapsed time. This suggested the importance of shortening treatment time. Recently, study by Nijkamp et al. shows that the diet and laxatives can reduce prostate motion during treatment [22]. The patients in this study had no special procedures to limit rectal filling, so our results represent an upper limit of therapeutic ratio which may be lower for patients who do use methods to control rectal volume. Also, a realistic margin would compensate for other uncertainties, such as errors in contouring, image registration, and position alignment.

Due to limited image datasets, only 10 treatment fractions were simulated in this study. The results of this study may be directly applied to hypo-fractionated treatment. However, care should be taken when extrapolating beyond our results, as a regularly fractionated prostate treatment may involve 35–40 fractions. In that case, we expect the target underdosing will be reduced if the motion is mostly random and the CTV definition in treatment is close to the mean position. However, if the target motion has a trend or the CTV definition is deviated from mean position, dose coverage would not improve with more fractions. To illustrate the change of accumulated dose during treatment course, Fig. 8 shows daily doses and accumulated doses of patient #6 for 10 fractions. The coverage is improved during the first three fractions and then stabilized after that.

Technologies such as EPIDs, CALYPSO, CBCT, and CT-on-rails allow accurate tracking of the target on a daily basis, and their use justifies reduction of the margin size. With no margins, the *IMRT Target* simulations essentially treated only the CTV. While there was underdosing in the seminal vesicles, satisfactory prostate dose was achieved for most patients. This result indicates that much smaller margins are justified around the prostate than the seminal vesicles, and that when treating prostate alone by this method, the size of the motion margin can be dictated only by the extent of intrafraction motion. For low risk patients, using implanted markers to locate the target each day can significantly reduce normal tissue dose while maintaining target coverage. For patients with high risk disease, the chance of microscopic or occult disease is increased. In the case of prostate patients, this is evidenced by extracapsular extension [23] and seminal vesicle involvement [24]. While the CTV–PTV margin has nominally accounted for target motion, its unintentional function has been to also treat these cells that are not traditionally included in the CTV. Therefore, this extremely conformal approach, which does not account for target rotations and deformations, is expected to be less successful in high risk patients.

Increasing levels of image guidance complexity provide more information with which to re-evaluate the treatment on a more frequent basis. The *CRT Re-plan* method using aperture change makes easy use of this information, as it simply shapes the blocks each day to the new PTV. After ten treatment fractions, the rectum dose from this method was very similar to that from the more standard *IMRT Bone* method. Also, Fig. 7 shows that all patients received adequate seminal vesicle dose and 8 of 9 patients received lower bladder dose by the CRT re-planning method. Though normal tissue sparing is limited by the convexity of the dose distribution and the penumbra size, this treatment provides very consistent target coverage. In reality, this treatment is not feasible in the absence of robust automatic contouring technology. However, since this method requires no further optimization, it is probably the least computationally intensive online adaptation that can be performed with this image data.

The most computationally intensive adaptation would involve a complete IMRT re-optimization of the original treatment plan. Compared to the *IMRT Bone* treatments, target coverage was main-
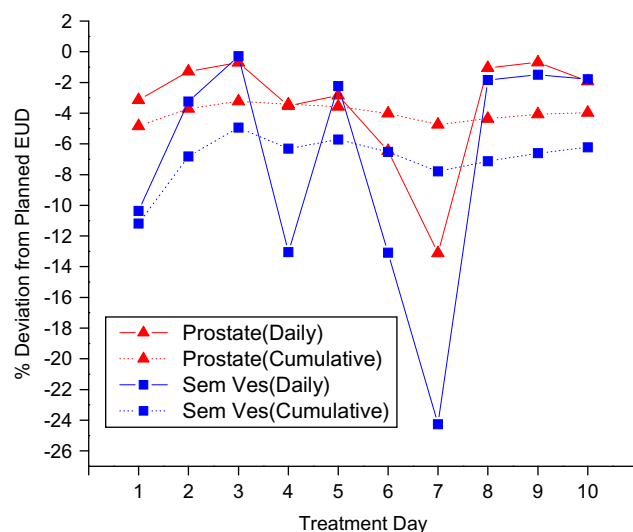

Fig. 8. Change of accumulated dose and daily dose through 10 fractions of patient #6.2.

tained for all patients, while bladder and rectum doses were, respectively, reduced by approximately 16% and 11%. This approach requires online ROI delineation and online plan re-optimization techniques. Although challenging, it is feasible to achieve these goals in the near future. We have developed an automatic ROI delineation method for HN images [15]. In principle, the same method can also be used on prostate images, but CBCT image quality is a major obstacle. In order to perform IMRT re-planning *online*, high performance computing techniques can be employed to accelerate computation. We were able to accelerate the deformable image registration speed by a factor close to the number of processing elements using a Beowulf cluster. Wu et al. showed that online IMRT re-optimization and MLC leaf conversion are achievable within 2–3 min [13].

In this study, we employed online IMRT re-planning approaches in which bladder and rectum volumes or walls were used as optimization constraints. The resulting difference between the two approaches, *IMRT Re-plan Volume* and *IMRT Re-plan Wall*, was shown to be small. When choosing OAR walls instead of the standard volumes, reduction of doses to bladder and rectum is limited to less than 1% on average, though using this approach does not drastically increase technical complexity. Extracting bladder and rectum walls from volumes would be straightforward, so it would be reasonable to employ the IMRT-wall approach for a small but cost-free improvement. This conclusion applies specifically to online re-planning methods, as any benefit from standard planning methods is expected to be negated by interfractional tissue shape changes.

An interesting result of this study is that IMRT techniques are much more sensitive to organ motion than CRT techniques. This is because the IMRT plan is more conformal, meaning that the dose gradient surrounds the target more tightly. Even with a 1-cm margin, underdoses in SV were still observed in several patients. Thus, regardless of margin size, high precision image guidance is more important in highly conformal treatment techniques. From this result, we would expect image guidance and intensity/energy modulation to be a decisive factor in proton prostate cancer treatments, where sharp dose gradients beyond the Bragg peak combined with particle penetration depth uncertainties create opportunities for significant dosimetric consequences.

We noticed that even in the online re-planning techniques, large discrepancies are shown between planning and accumulated

bladder and rectum doses. This encourages a close-loop adaptive treatment technique with dose tracking, in which the re-planning takes account of accumulated dose up to that point in the treatment course [25,26]. Otherwise, while OAR doses may meet constraints in treatment planning, they are likely over the limits in actual treatments.

Conclusions

Online treatment plan re-optimization may significantly improve therapeutic ratio in prostate cancer treatments when seminal vesicle is involved mostly due to the reduction of PTV margin. However for low risk patient with only prostate involved, online target alignment IMRT treatment would achieve similar results as online re-planning. For all IGRT approaches, the delivered organ-at-risk doses may be significantly different from treatment planning prediction.

Acknowledgement

References

[1] Beltran C, Herman MG, Davis BJ. Planning target margin calculations for prostate radiotherapy based on intrafraction and interfraction motion using four localization methods. Int J Radiat Oncol Biol Phys 2008;70:289–95.

[2] Schaly B, Bauman GS, Song W, Battista JJ, Van DJ. Dosimetric impact of image-guided 3D conformal radiation therapy of prostate cancer. Phys Med Biol 2005;50:3083–101.

[3] Ling CC, Yorke E, Fuks Z. From IMRT to IGRT: frontierland or neverland? Radiother Oncol 2006;78:119–22.

[4] Herman MG. Clinical use of electronic portal imaging. Semin Radiat Oncol 2005;15:157–67.

[5] Jans HS, Syme AM, Rathee S, Fallone BG. 3D interfractional patient position verification using 2D–3D registration of orthogonal images. Med Phys 2006;33:1420–39.

[6] Stutzel J, Oelfke U, Nill S. A quantitative image quality comparison of four different image guided radiotherapy devices. Radiother Oncol 2008;86:20–4.

[7] Guckenberger M, Meyer J, Wilbert J, Baier K, Sauer O, Flentje M. Precision of image-guided radiotherapy (IGRT) in six degrees of freedom and limitations in clinical practice. Strahlenther Onkol 2007;183:307–13.

[8] Yue NJ, Knisely JP, Song H, Nath R. A method to implement full six-degree target shift corrections for rigid body in image-guided radiotherapy. Med Phys 2006;33:21–31.

[9] Chung PW, Haycocks T, Brown T, Cambridge Z, Kelly V, Alasti H, et al. On-line aSi portal imaging of implanted fiducial markers for the reduction of interfraction error during conformal radiotherapy of prostate carcinoma. Int J Radiat Oncol Biol Phys 2004;60:329–34.

[10] Wertz H, Lohr F, Dobler B, Mai S, Welzel G, Boda-Heggemann J, et al. Dosimetric consequences of a translational isocenter correction based on image guidance for intensity modulated radiotherapy (IMRT) of the prostate. Phys Med Biol 2007;52:5655–65.

[11] Ding GX, Duggan DM, Coffey CW, Deeley M, Hallahan DE, Cmelak A, et al. A study on adaptive IMRT treatment planning using kV cone-beam CT. Radiother Oncol 2007;85:116–25.

[12] Feng Y, Castro-Pareja C, Shekhar R, Yu C. Direct aperture deformation: an interfraction image guidance strategy. Med Phys 2006;33:4490–8.

[13] Wu QJ, Thongphiew D, Wang Z, Mathayomchan B, Chankong V, Yoo S, et al. On-line re-optimization of prostate IMRT plans for adaptive radiation therapy. Phys Med Biol 2008;53:673–91.

[14] Wu C, Jeraj R, Olivera GH, Mackie TR. Re-optimization in adaptive radiotherapy. Phys Med Biol 2002;47:3181–95.

[15] Zhang T, Chi Y, Meldolesi E, Yan D. Automatic delineation of on-line head-and-neck computed tomography images: toward on-line adaptive radiotherapy. Int J Radiat Oncol Biol Phys 2007;68:522–30.

[16] Langen KM, Jones DT. Organ motion and its management. Int J Radiat Oncol Biol Phys 2001;50:265–78.

[17] Orton NP, Tome WA. The impact of daily shifts on prostate IMRT dose distributions. Med Phys 2004;31:2845–8.

[18] Yan D, Jaffray DA, Wong JW. A model to accumulate fractionated dose in a deforming organ. Int J Radiat Oncol Biol Phys 1999;44:665–75.

[19] Ghilezan M, Yan D, Liang J, Jaffray D, Wong J, Martinez A. Online image-guided intensity-modulated radiotherapy for prostate cancer: how much improvement can we expect? A theoretical assessment of clinical benefits and potential dose escalation by improving precision and accuracy of radiation delivery. Int J Radiat Oncol Biol Phys 2004;60:1602–10.

[20] Beltran C, Herman MG, Davis BJ. Planning target margin calculations for prostate radiotherapy based on intrafraction and interfraction motion using four localization methods. Int J Radiat Oncol Biol Phys 2007.

[21] van Herk M, Remeijer P, Lebesque JV. Inclusion of geometric uncertainties in treatment plan evaluation. Int J Radiat Oncol Biol Phys 2002;52:1407–22.

[22] Nijkamp J, Pos FJ, Nuver TT, de JR, Remeijer P, Sonke JJ, et al. Adaptive radiotherapy for prostate cancer using kilovoltage cone-beam computed tomography: first clinical results. Int J Radiat Oncol Biol Phys 2008;70:75–82.

[23] Chao KK, Goldstein NS, Yan D, Vargas CE, Ghilezan MI, Korman HJ, et al. Clinicopathologic analysis of extracapsular extension in prostate cancer: should the clinical target volume be expanded posterolaterally to account for microscopic extension? Int J Radiat Oncol Biol Phys 2006;65:999–1007.

[24] Kestin L, Goldstein N, Vicini F, Yan D, Korman H, Martinez A. Treatment of prostate cancer with radiotherapy: should the entire seminal vesicles be included in the clinical target volume? Int J Radiat Oncol Biol Phys 2002;54:686–97.

[25] Birkner M, Yan D, Alber M, Liang J, Nusslin F. Adapting inverse planning to patient and organ geometrical variation: algorithm and implementation. Med Phys 2003;30:2822–31.

[26] Wu Q, Liang J, Yan D. Application of dose compensation in image-guided radiotherapy of prostate cancer. Phys Med Biol 2006;51:1405–19.